The Proton and Neutron as Distortional Structures in the Geometric Manifold

Dale. R. Koehler (drkoehler.koehler@gmail.com)
Sandia National Laboratories

Research Article

Keywords: Classical field theory, Classical mechanics, General relativity, Geometry, Nuclear Physics, Structural stability

Posted Date: September 30th, 2021

DOI: https://doi.org/10.21203/rs.3.rs-949816/v1

The Proton and Neutron as Distortional Structures in the Geometric Manifold

Dale. R. Koehler*

Sandia National Laboratories (retired)

82 Kiva Place, Sandia Park, NM 87047

Email address: drkoehler.koehler@gmail.com

Telephone No. (505) 273-3570

***Abstract*— It is shown in the present work that the distorted-space model of matter as extended to mimics of the proton and neutron can be described as muonic-based structures. These distorted-geometry structures exhibit non-Newtonian features wherein the hole or core-region fields of the structure (negative pressure core for a positive-charge positive-pressure large-r structure) do not behave functionally in a r^{-4} manner and terminate at zero at the radial origin (no singularity). Of particular interest is that of r^{-6} energy-density behavior at structural radial distances near the core of the distortion, a region also displaying potential-well behavior.**

Ketwords—Classical field theory; Classical mechanics; General relativity; Geometry; Nuclear Physics; Structural stability

1. INTRODUCTION

For this distorted-geometry (DG) modeling, we maintain and expand the geometrical perspectives inherent in the "Curved empty space as the building material of the physical world" supposition of Clifford [1];

"RIEMANN has shewn that as there are different kinds of lines and surfaces, so there are different kinds of space of three dimensions; and that we can only find out by experience to which of these kinds the space in which we live belongs. In particular, the axioms of plane geometry are true within the limits of experiment on the surface of a sheet of paper, and yet we know that the sheet is really covered with a number of small ridges and furrows, upon which (the total curvature not being zero) these axioms are not true. Similarly, he says, although the axioms of solid geometry are true within the limits of experiment for finite portions of our space, yet we have no reason to conclude that they are true for very small portions; and if any help can be got thereby for the explanation of physical phenomena, we may have reason to conclude that they are not true for very small portions of space.

I wish here to indicate a manner in which these speculations may be applied to the investigation of physical phenomena. I hold in fact

(1) That small portions of space are in fact of a nature analogous to little hills on a surface which is on the average flat; namely, that the ordinary laws of geometry are not valid in them.

(2) That this property of being curved or distorted is continually being passed on from one portion of space to another after the manner of a wave.

(3) That this variation of the curvature of space is what really happens in that phenomenon which we call the motion of matter, whether ponderable or etherial.

(4) That in the physical world nothing else takes place but this variation, subject (possibly) to the law of continuity.

A quote from Wheeler's work [2] published in 1955 reads; *"In the 1950's, one of us [3] found an interesting way to treat the concept of body in general relativity. An object can in principle be constructed out of gravitational radiation or electromagnetic radiation, or a mixture of the two, and may hold itself together by its own gravitational attraction…A collection of radiation held together in this way is called a geon (a gravitational electromagnetic entity) and is a purely classical object….In brief, a geon is a collection of gravitational or electromagnetic energy, or a mixture of the two, held together by its own gravitational attraction, that describes mass without mass."*

Subsequently at *The International Congress for Logic, Methodology, and Philosophy of Science* in 1960, he [4] began by quoting William Kingdon Clifford's [1] "Space-Theory of Matter" of 1870 and stated *"The vision of Clifford and Einstein can be summarized in a single phrase, 'a geometrodynamical universe': a world whose properties are described by geometry, and a geometry whose curvature changes with time – a dynamical geometry."*

A comprehensive and general treatment of the historical, geometric and physical foundations of modern geometrodynamics is found in the already cited publications of Wheeler [2-4]. Additional work in this field continues, some of which is cited in references [5-10]. The present distorted-geometry treatment departs from these cited "geon constructional methods" in that we do not constrain the distortional descriptions to only gravitational coupling-constant produced structures.

The classical Riemannian four-dimensional curvature equations have been applied to describe the "localized geometrical distortions and associated energy distributions" at both quantum- and galactic-level magnitudes and radial-extensions. By requiring that the geometric distortions mimic the physical characteristics of the elementary particles, a coupling constant between energy and geometry is produced. The theoretical modeling and calculational procedure is limited to those geometric-distortional families satisfying an equation-of-state, which also expresses static, spherically-symmetric Maxwellian tensor behavior.

Functional solutions to Riemann's geometric, non-linear, coupled, partial-differential equations have classically not been forthcoming. A solution however has been found for the Riemannian equation-set by describing the "distorted" space as satisfying the “equation of state”, Eq.(1). The Riemannian field equations, produced by the present “metric-solution”, Eq.(2), are of such a character that, over portions of the radial extensions of the distortion, the geometrical tensor elements exhibit negative, as well as positive, curvature-magnitudes and energy-densities. The field-observable in the negative energy-density (negative pressure) spatial region (the core region) is non-Coulombic and non-infinite at the radial origin. Mass, electric charge and magnetic moments have been simulated for the down-quark, up-quark, electron, tauon, muon and neutrino as well as for a hypothetical beta-decay transition-mediating distortion-particle; this process also generates a geometric expression for the Fermi constant [11] and conversely predicts a mass-value for the W-boson calculated to the precision of the electron g-factor (gyromagnetic ratio).

Figure 1 displays the field energy-density quantities for three of these particle structures.

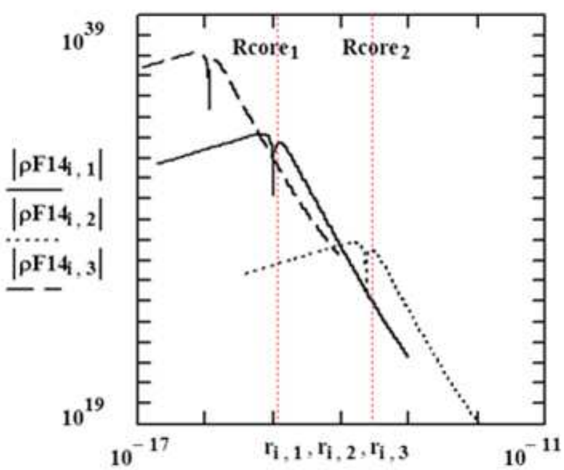

Fig. 1 Electric-Field energy-density distribution function for distortion-1 ≡ down_quark (mass-energy = 9.269 me*c^2), distortion-2 ≡ electron and distortion_3 ≡ muon (mass-energy = 206.768 me*c^2) where $\boldsymbol{\rho F14} \equiv \boldsymbol{Fd_{14}^{\,2}}$ (see Eqs 12-15); logarithmic ordinate in J/m^3 units and logarithmic abscissa in meters.

The dependence of the field quantities on mass-energy and electric-charge is apparent in the Figure. The field energy-density magnitudes should be compared with the experimental data in reference [17].

By incorporating gravitational-field structures into the geometric modeling and simulation process, a refined coupling-constant is engendered. This process recovers the gravitational coupling-constant of general relativity and leads to a structural description of gravitational-like geometric-distortions.

We showed in [11] that the propagation velocity in the core region (negative pressure core for a positive-charge, positive-pressure (at large-r) structure) of these distorted-geometry (DG) structures was approximately 1.5 times that external to the core; see Fig.2. This feature, which is a fundamental attribute of such structures, is equivalent to a “partial light trapping” phenomenon and for gravitational structures would be classically associated with “black holes”.

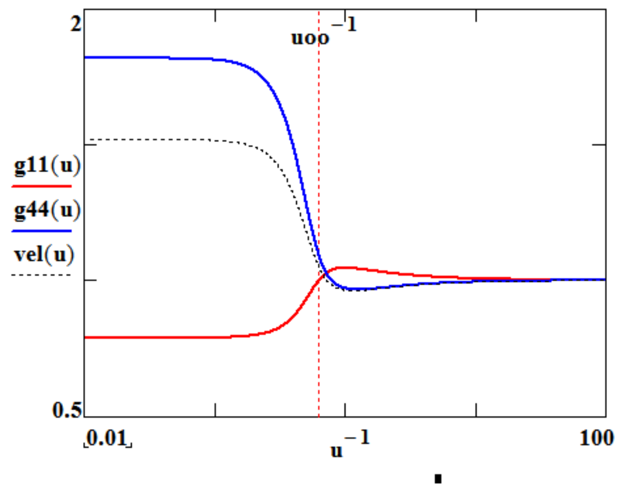

Fig.2 Metrics and propagation-velocity factor for an electron structure; .uoo = 1.27394.

A “geometric maximum-energy-density” feature was successfully exploited to geometrically explain and quantify the Fermi constant [11]; in addition a “*stability-based minimum-energy-density*” condition was fundamental to describing the structure of the “stable DG electron” feature. Energy-densities are equivalent to pressures and the core and shell regions of the structure hold the system in stable equilibrium. Fig.3 graphically displays such structures.

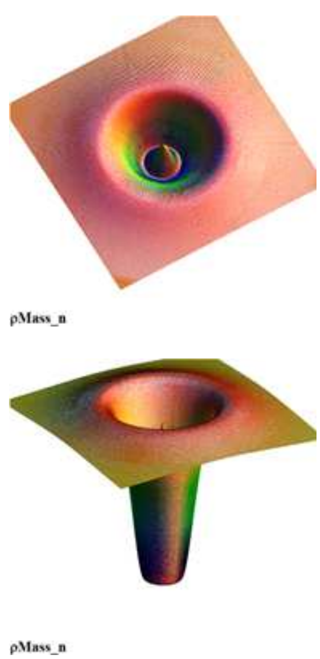

Fig.3 Mass-Energy-Density distribution-function surface-plots (two views) (linear radii and logarithmic amplitudes) for the geometric electron distortion.

In the perspective of [11], the DG model is a departure from the classical geometry model where the Einstein Curvature-tensor is the stress-energy-tensor describing the "material contents" of the energy distribution. The DG model is rather viewed with the energy-content residing in the warping or distorting of the manifold and therefore in its geometric-tensors, and the "curved empty space" [11] referred to above is a "localized curved or distorted space" devoid of an "external or foreign" causative matter-entity.

2. THEORETICAL FOUNDATION

A "constitutive relation" or "equation-of-state" was used as descriptive of the distorted-space volume (the physical spatial volume encompassing the distortion-produced energy), that is,

$$\boldsymbol{Td_4^4} = -\boldsymbol{Td_1^1} - \boldsymbol{Td_2^2} - \boldsymbol{Td_3^3} \quad and \quad \boldsymbol{Td_3^3} = \boldsymbol{Td_2^2}. \tag{1}$$

This description, Eq.(1), of the *distorted-space volume*, has led to the *universal structural solution,* Eq.(2), (see Eqs. (5)-(9) for variable definitions) for the fundamental Riemann geometric-equation-set, Eqs.4.

$$\mu' = \frac{2(1-u^3)u^2}{(Iu-\gamma)R0} \tag{2}$$

where the metric quantities $g_{11} \equiv -e^{\mu}$ and $g_{44} \equiv e^{\nu}$; $\nu' = \left[-2+\frac{1}{1-u^3}\right]\mu'$

and the transformed radial variable $u \equiv \frac{R0}{r}$;

$$Iu = -u\left[\frac{3}{7}u^6 - \frac{3}{4}u^3 + 1\right]. \tag{3}$$

Riemann's geometric equations (Tolman [13]), presented here as Eqs.(4), are expressed in the metric-variables μ' and ν' and the manifestation of the composite coupling-constant appears in the geometric quantities γ and the geometric "transformation radius" *R0,* both determined from the "distorted spatial volume" with electromagnetic and/or gravitational energy-density components.

$$8\pi\kappa\mathbf{T_1^1} = -e^{-\mu}\left[\frac{\mu'^2}{4} + \frac{\mu'\nu'}{2} + \frac{\mu'+\nu'}{r}\right] + e^{-\nu}\left[\ddot{\mu} + \frac{3}{4}\dot{\mu}^2 - \frac{\dot{\mu}\dot{\nu}}{2}\right],$$

$$8\pi\kappa\mathbf{T_2^2} = -e^{-\mu}\left[\frac{\mu''}{2} + \frac{\nu''}{2} + \frac{\nu'^2}{4} + \frac{\mu'+\nu'}{2r}\right] + e^{-\nu}\left[\ddot{\mu} + \frac{3}{4}\dot{\mu}^2 - \frac{\dot{\mu}\dot{\nu}}{2}\right] =$$

$$= 8\pi\kappa T_3^3,$$

$$8\pi\kappa\mathbf{T_4^4} = -e^{-\mu}\left[\mu'' + \frac{\mu'^2}{4} + \frac{2\mu'}{r}\right] + e^{-\nu}\left[\frac{3}{4}\dot{\mu}^2\right],$$

$$8\pi\kappa\mathbf{T_4^1} = +e^{-\mu}\left[\dot{\mu}' - \frac{\dot{\mu}\nu'}{2}\right],$$

$$8\pi\kappa\mathbf{T_1^4} = -e^{-\nu}\left[\dot{\mu}' - \frac{\dot{\mu}\nu'}{2}\right]. \tag{4}$$

While the "energy-density Equation-of-state" Eq. (1) is equivalent to Maxwell's "energy-density" form for static, spherically-symmetric Maxwellian tensor behavior [11,13], the field equations, in both the EM realm and the gravitational realm (Q = 0), exhibit r^{-6} geometric, static, spherically-symmetric Maxwellian tensor behavior which we have interpreted as constituting a "magnetic monopole" mimic (what is a "magnetic monopole"?).

Building on the earlier work, [11, 12], we apply the geometric concepts to produce a proton- and neutron-conglomerate of distortional-geometric muon-mimics.

This section is a brief summary of the development in [11] and is included here as a less cumbersome introduction or reference to the theoretical modeling concepts.

Symbols [11] are

$$uB0(S=1, Q=3) \equiv \frac{R0}{ro} = 1.6,$$

$$uB0(S=1/2, Q=3) \equiv \frac{R0}{ro} = 1.239. \tag{5}$$

R0 is the geometric transformation radius ($R0_{electron}$ is calculated from the fundamental-particle magnetic-field component) and *ro* is the radial value at which the energy-density distribution-function transitions from the core-value to its negative in the shell ($r \to \infty$) region; $ro \equiv \frac{R0}{uo}$ follows from solution for the *uo* roots of the field equations (Eqs.(6))

$$(1-3u^3)(1-u^3)^2 - 4u^2(Iu-\gamma) = 0 \text{ for } \boldsymbol{Td_2^2},$$

$$(1-3u^3)(1-u^3)(1-2u^3) - 6u^2(Iu-\gamma) = = 0 \text{ for } \boldsymbol{Td_4^4} \text{ and}$$

$$(1-3u^3)(1-u^3)u^3 + 2u^2(Iu-\gamma) = = 0 \text{ for } \boldsymbol{Td_1^1} + \boldsymbol{Td_2^2}. \tag{6}$$

We also define

$$\gamma \equiv \frac{2\,R0}{Rs} \quad and \quad Rs \equiv \text{Schwarzschild radius} = 2\,\kappa\,Mc^2 \tag{7}$$

$$where \quad \kappa \equiv \kappa G + \kappa o = Gc^{-4} + \frac{\alpha\,\hbar c\left(\frac{Q}{3}\right)^2}{2(Mc^2)^2}.$$

For the electron we write (me ≡ mass electron, Q_{elec} = 3),

$$ro(electron) = \frac{\beta(1/2,3)}{uB0(1/2,3)}\frac{\hbar c}{me\,c^2}, \tag{8}$$

$$\text{with } \beta(S,Q) = \left[\frac{2}{3}\alpha\left(\frac{g_e}{2}S\frac{Q}{3}\right)^2\right]^{\frac{1}{3}},$$

α = fine structure constant, S is the spin quantity and

g_e is the gyromagnetic ratio factor. Then,

$$ro_{geo\_max} = ro(electron) = 3.3297(10)^{-14} \text{ meters.} \tag{9}$$

The core-radii for the EM structures are inversely proportional to the mass-energy of the distorted-geometry-structures and therefore it follows that the ro radius for the muon, or anti-muon, is

$$ro(muon) = \frac{me\,c^2}{m_{muon}\,c^2}ro(electron) = 1.61(10)^{-16} \text{ meters.} \tag{10}$$

In the earlier development [11] for the geometric Fermi-constant, *GF* is $GF_{geo} \stackrel{\text{def}}{=} \left[fe\,\frac{4\pi}{3}R0^3\right]MW$ and MW = mass-energy of the W^-boson. The quantity, $fe = \frac{3}{2}\left(\frac{\pi}{2}\right)^2$, was originally introduced as a volume-adjustment-factor in this derivation.

The *uo* root values ($uo \equiv \frac{R0}{ro}$), for determining *ro* values, from Eqs.(6), are plotted in Fig.4

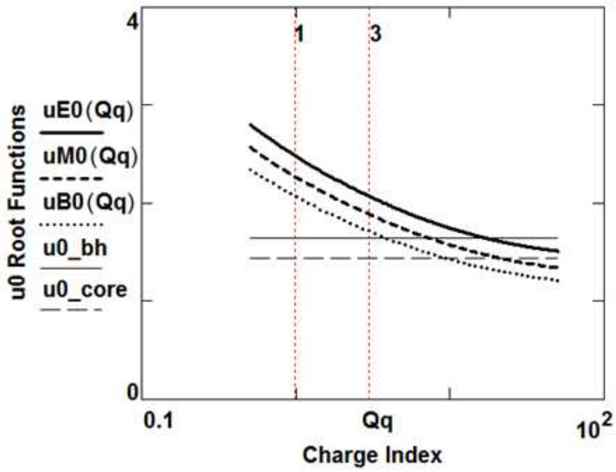

Fig. 4 Radial-zero functions u_0 (from Eqs.(6)) relative to electric-charge values; *uE0* for the electrical $\boldsymbol{Td^2_2}$ function, *uM0* for the mass-energy-density $\boldsymbol{Td^4_4}$ function and *uB0* for the magnetic-energy-density $\boldsymbol{Td^1_1 + Td^2_2}$ function. Abscissa charge-values are displayed as a function of the index *Qq*. *uo(Qq)* is graphically used for the zero-radial-function *uo*. Also indicated is the E_field quantity, *u0_core = uE0(Qq* = 0), and a gravitational "black-hole *u0_bh*" value.

The radial zero of the gravitational field quantities expressed in Eqs.(6) is *u(ro)* = 3.27512/2 if $ro = Rs_{geo}$. $Rs_{geo} = R0_{geo}/u(ro)$ is the geometric manifestation of the Schwarzschild "metric-radial-zero", the radial singularity classically interpreted as a "black-hole" radius.

The Riemannian geometric field equations follow from Eq.(4) and are taken from [13] according to Tolman;

"For the presently described spherically symmetric Maxwellian case, ϕ, the electrostatic potential, is a function of r alone, and the Maxwellian electromagnetic tensor and the associated field tensor $\boldsymbol{F_{1\mu}}$ *can be constructed according to my equation (5), where the only surviving field tensor components are"*

$$\mathbf{F_{21} = -F_{12}\ ,\ F_{13} = -F_{31}} \quad \text{and} \quad \mathbf{F_{14} = -F_{41}}\ , \qquad \text{i.e.}$$

$$\mathbf{T^{\mu\nu} = -g^{\nu\beta}F^{\mu\alpha}F_{\beta\alpha} + \frac{1}{4}g^{\mu\nu}F^{\alpha\beta}F_{\alpha\beta}} \quad \text{or}$$

$$\mathbf{T^{\mu\mu} = -g^{\mu\mu}F^{\mu\alpha}F_{\mu\alpha} + \frac{1}{4}g^{\mu\mu}F^{\alpha\beta}F_{\alpha\beta}}\ , \quad \text{then}$$

$$\mathbf{T^4_4 = \frac{(F_{12}F^{12} + F_{13}F^{13} - F_{14}F^{14})}{2}}\ , \quad \mathbf{T^1_1 = \frac{(-F_{12}F^{12} - F_{13}F^{13} - F_{14}F^{14})}{2}}\ ,$$

$$\mathbf{T^2_2 = \frac{(-F_{12}F^{12} + F_{13}F^{13} + F_{14}F^{14})}{2}} \quad \text{and} \quad \mathbf{T^3_3 = \frac{(F_{12}F^{12} - F_{13}F^{13} + F_{14}F^{14})}{2}}\ . \qquad (11)$$

The resultant field quantities are

$$\mathbf{(F_{14})^2 = -\left(T^4_4 + T^1_1\right)g_{11}\,g_{44} = \left(T^2_2 + T^3_3\right)g_{11}\,g_{44}}\ ,$$

$$\mathbf{(F_{12})^2 = -\left(T^2_2 + T^1_1\right)g_{11}\,g_{11}} \ \textbf{and} \ \mathbf{(F_{13})^2 = -\left(T^3_3 + T^1_1\right)g_{11}\,g_{11}}\ . \qquad (12)$$

Therefore, we see that the static-spherically-symmetric Maxwellian tensors exhibit the same stress and energy relationship as the geometric tensors.

Finally, it is of interest to examine the ratio of the $1/r^6$ tensor-component to the $1/r^4$ tensor-component in the construction of the geometric fields. The geometric-energy-density or field equations [13] are (the "***d***" symbolism denotes the "***distorted space***" modeling)

$$8\pi\kappa\, \boldsymbol{Td^1_1} = -e^{-\mu}\frac{1}{(\mathrm{Iu}-\gamma)}\left(\frac{u^2}{R0}\right)^2\left[2\,u^2 + (3\,u^3 - 1\,)\,\frac{1-u^3}{(\mathrm{Iu}-\gamma)}\right],$$

$$8\pi\kappa\, \boldsymbol{Td^2_2} = e^{-\mu}\frac{1}{(\mathrm{Iu}-\gamma)}\left(\frac{u^2}{R0}\right)^2\left[4\,u^2 + (3u^3 - 1\,)\frac{(1-u^3)^2}{(\mathrm{Iu}-\gamma)}\right],$$

$$\text{and} \quad 8\pi\kappa\,(\,\boldsymbol{Td^2_2} + \boldsymbol{Td^1_1}\,) =$$

$$= e^{-\mu}\frac{1}{(\mathrm{Iu}-\gamma)}\left(\frac{u^2}{R0}\right)^2\left[2\,u^2 - (3u^3 - 1\,)\frac{(1-u^3)u^3}{(\mathrm{Iu}-\gamma)}\right] \qquad (13)$$

leading to

$$(\boldsymbol{Fd_{14}})^2 = -g_{11}g_{44}\left(\boldsymbol{Td^4_4} + \boldsymbol{Td^1_1}\right) = g_{11}g_{44}\left(\,2\,\boldsymbol{Td^2_2}\,\right) \quad \text{and}$$

$$(\boldsymbol{Fd_{14}})^2(\mathrm{r}\to\infty) \stackrel{\text{def}}{=} \left(\frac{\mathrm{Rs}}{2}\right)^2\frac{2}{8\pi\kappa}\,\frac{1}{\mathrm{r}^4} = \frac{\mathrm{Rs}^2}{2}\,\frac{1}{8\pi\kappa}\,\frac{1}{\mathrm{r}^4} \stackrel{\text{def}}{=} \left(\frac{\mathrm{q}}{4\pi\varepsilon o\,\mathrm{r}^2}\right)^2\frac{\varepsilon o}{2} . \quad (14)$$

$$(\boldsymbol{Fd_{12}})^2 + (\boldsymbol{Fd_{13}})^2 = 2\,g_{11}g_{11}\left(\frac{\boldsymbol{Td^4_4} - \boldsymbol{Td^1_1}}{2}\right) \stackrel{\text{def}}{=} \boldsymbol{Fd_{mag}}^2 =$$

$$= -2\,g_{11}g_{11}\left(\boldsymbol{Td^1_1} + \boldsymbol{Td^2_2}\right) \quad \text{and}$$

$$(\boldsymbol{Fd_{12}})^2 + (\boldsymbol{Fd_{13}})^2(r\to\infty) = 2\,\mathrm{Rs}\,\mathrm{R0}^3\frac{1}{8\pi\kappa}\,\frac{1}{\mathrm{r}^6} \stackrel{\text{def}}{=}$$

$$\stackrel{\text{def}}{=} \frac{\mu o}{2}\left(\frac{\mu_{spin}}{2\pi}\right)^2\frac{1}{\mathrm{r}^6} \qquad (15)$$

where

$$\mu\_spin \stackrel{\text{def}}{=} \left(\frac{g_e}{2}\frac{Qe}{3M}\right) S\,\hbar \quad \text{and} \quad g_e = 2.0023193043\,6\ .$$

In discussions of the negative energy-density (pressure) core-regions of this universal (EM as well as gravitational) distorted-geometry structure, it should be emphasized that a negative energy-density gravitational feature (a repulsive gravitational force or negative pressure) is non-Newtonian. The hole or core region-fields of the structure are repulsive thereby stabilizing the structure, do not behave functionally in an r^{-4} manner and terminate at zero at the radial origin (no singularity). This field behavior is a fundamental feature of these "distorted-space" structures; the field exhibits r^{-4} , r^{-6} and r^{-n} dependences in both the core and shell regions and is thereby able to account for "Newtonian"-, "weak"- and "strong-fields"(see Eqs.(14,15)).

To further illustrate the structural character of the "distortional-geometry mimics", we compare at "near-core radial regions" the geometrostatic field quantities $Fd_{14}{}^2$ and $Fd_{mag}{}^2$ which are also the geometric mimics of the Maxwellian tensors. For both gravitational and electromagnetic distortions, the magnetic field component, $Fd_{mag}{}^2$, is non-zero at the "radial field zero", $Fd_{14}{}^2 = 0$, or "core radius (*ro*)" (in the gravitational realm, this field feature would seem responsible for accretion-disk and galaxy-matter rotational-distribution behavior). Figures 5 and 6 are constructed for the "distorted-space electron-mimic" although the energy-density distribution functions are qualitatively similar in the normalized radial variable $u = \frac{R0}{r}$. The Figures are meant to more dramatically illustrate the magnitude of the structure's magnetic energy-density component vs the $Fd_{14}{}^2$ energy-density component.

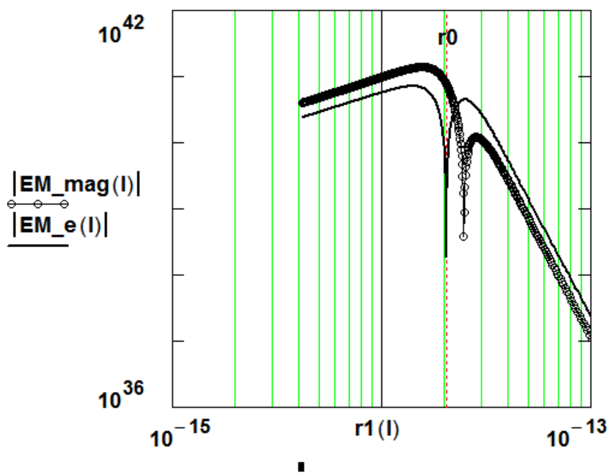

Fig.5 Field-Energy-Density distribution-functions; radii (logarithmic in meters) and amplitudes (logarithmic in joules/m^3) for the DG_geometric electron-distortions. EM_mag ≡ $Fd_{mag}{}^2(\boldsymbol{electron})$ and EM_e ≡ $Fd_{14}{}^2(\boldsymbol{electron})$.

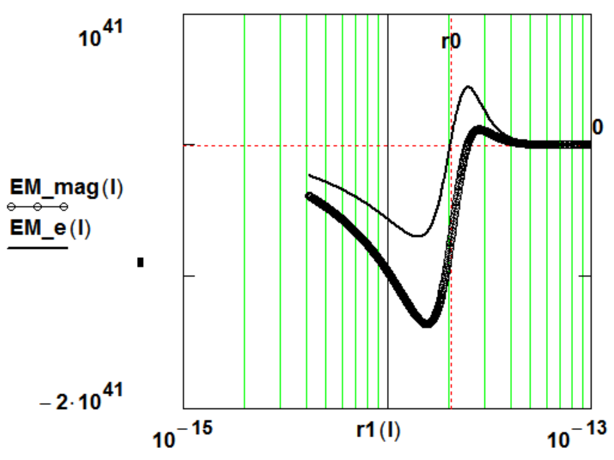

Fig.6 Field-Energy-Density distribution-functions; radii (logarithmic in meters) and amplitudes (linear in joules/m^3) for the DG_geometric electron-distortions. EM_mag ≡ $Fd_{mag}{}^2(\boldsymbol{electron})$ and EM_e ≡ $Fd_{14}{}^2(\boldsymbol{electron})$.

Actually, the $Fd_{14}{}^2$ fields contain r^{-6} elements of a magnitude comparable to the magnetic-field strengths $Fd_{mag}{}^2$, resulting in a significant departure from the classical Newtonian r^{-4} (or r^{-6}) behavior. The fields also exhibit potential-well behavior as they radially (shell values) transition to repulsion (if attractive in the shell) at the hole-core radius *ro*.

3. PROTON AND NEUTRON MODELING

We use the following experimental data [14-16] to generate and illustrate the model parameters:
mass energy of proton (*Mp*) = 938.2716 MeV, electric charge of proton (*Qp*) = +e and gyromagnetic ratio (*g*-factor) of **proton (*gp*) = 5.585694**;

mass energy of neutron (*Mn*) = 939.564 MeV, electric charge of neutron (*Qn*) = 0, gyromagnetic ratio (*g*-factor) of **neutron (gn) = -3.826085**;

mass energy of muon (*Mμ*) = 105.658 MeV, electric charge of muon (*Qμ*) = -e, gyromagnetic ratio (*g*-factor) of **muon (*gμ*) = -2.002331**, and

mass-energy of anti-muon (*Maμ*) = 105.658 MeV = *Mμ*, , electric charge of anti-muon (*Qaμ*) = +e and gyromagnetic ratio (*g*-factor) of **anti-muon (*gaμ*) = 2.002331**.

The electron characteristics are;
mass energy of electron ($me{*}c^2$) = 0.510998 MeV, electric charge of electron (*Qe*) = *-e*, gyromagnetic ratio (*g*-factor) of **electron (*ge*) = -2.002319**.

Calculating the binding energy of the **proton**, modeled as a structure of **4 muons and 5 anti-muons**, we get BEp (binding energy of proton) ≡ 9 *Mμ – Mp* = 12.6504 MeV. Similarly, the binding energy of the **neutron** ≡ Ben = 9 *Mμ* + *Me* – *Mn* = 11.358 MeV. The muons and anti-muons are posited to coexist within the immediate field environment of the composite structure as, for example, neutrons existing within elemental structures, or, in other field-induced [15,16] modifications. For comparison to other nuclear structures, a binding energy per nucleon, where a "nucleon" definition here incorporates the muon, is BEp_μ = 1.40555 MeV/nucleon and Ben_μ = 1.318666 MeV/nucleon.

For the DG_mimicked-proton, the electric-field is that of an anti-muon (the other 4 muon/anti-muon pairs exhibiting zero-charge or self-neutralization [16] and zero *g*-factors). The *g*-factor value of the 4th muon is field "flipped" and a resultant sub-structure of two anti-muons and the "flipped" muon-produces a "field induced" composite *g*-factor, reduced from the free-field value of (2.002331) per anti-muon to (1.861898) per anti-muon, to create a **proton *g*-factor** of **(5.585694)**. The proton (stacked-muon) radius, assuming a 3-layer, 3 muon/layer, @ 4 *ro*-muon separation (center to center) between muons, in a stacked-geometry-configuration, would be approximately 10 *ro*_muon or 1.0625(10)$^{-15}$ meters.

For the DG-mimicked-neutron, which is here posited as a DG-mimicked proton surrounded by a DG-mimicked electron (ge = -2.002319), the simplest formation structure would be that of field "flipping" the g-factor of one DG-proton-anti-muon from (+2.002331) to (-2.002331) with a field induced reduction to (-1.823766). The resultant **neutron *g*-factor** would then be **(-1.823766) + (-2.002319) = (-3.826085)**.

For this DG_mimicked-neutron, the electric-field is that of the DG_mimicked core-proton plus the field of the shroud DG_mimicked electron registered on the same center as the protonic-core (see Fig.7). In other words, a zero-charge field (at large radii) but a "DG-field" near and within the ro(electron) radius. The neutron ro radius is that of the shroud-electron-mimic or ro(neutron) = ro(shroud-electron) = $2.197(10)^{-14}$ meters.

The energy-density features of these structures are illustrated in Fig. 7. The field-energy-density distribution functions are recast as, for example,

$$\boldsymbol{U\_pro(r)} \equiv (\boldsymbol{Fd_{14}})^2 = -g_{11}g_{44}\left(\boldsymbol{Td_4^4} + \boldsymbol{Td_1^1}\right) = g_{11}g_{44}\left(\boldsymbol{2\,Td_2^2}\right)$$

and the neutron distribution is defined as

$$\boldsymbol{U\_neu(r) \equiv U\_pro_n(r)\ -U\_elec_n(r)}$$

where the "n" subscript denotes the impact of the gyromagnetic factor ge. The DG_proton g-factor produces ***U_pro(r) + U_elec(r)*** and the DG_neutron g-factor produces ***$U\_pro_n(r)$* + *$U\_elec_n(r)$***. Absolute values are displayed because of the energy-density-value transition at the core radii.

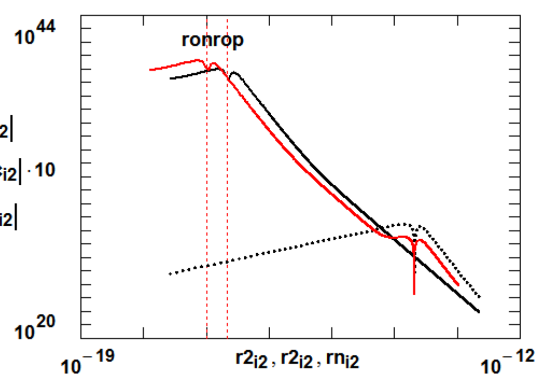

Fig.7 Field-Energy-Density distribution-functions; radii (logarithmic in meters) and amplitudes (logarithmic in joules/m^3) for the DG_geometric distortions ***U_pro(r), U_elec(r)*** and ***U_neu(r).***

The symbols ron and rop are the DG_neutron and DG_proton core radii.

Some experimental data have been measured for the proton and is detailed in reference-[17] as;

"The proton, one of the components of atomic nuclei, is composed of fundamental particles called quarks and gluons. Gluons are the carriers of the force that binds quarks together, and free quarks are never found in isolation—that is, they are confined within the composite particles in which they reside. The origin of quark confinement is one of the most important questions in modern particle and nuclear physics because confinement is at the core of what makes the proton a stable particle and thus provides stability to the Universe. The internal quark structure of the proton is revealed by deeply virtual Compton scattering, a process in which electrons are scattered off quarks inside the protons, which subsequently emit high-energy photons, which are detected in coincidence with the scattered electrons and recoil protons. Here we report a measurement of the pressure distribution experienced by the quarks in the proton. We find a strong repulsive pressure near the centre of the proton ***(up to 0.6 femtometres)*** *and a binding pressure at greater distances. The average* ***peak pressure near the centre is about 10^{35} Pascals (Joule/m^3)***, *which exceeds the pressure estimated for the most densely packed known objects in the Universe, neutron stars. This work opens up a new area of research on the fundamental gravitational properties of protons, neutrons and nuclei, which can provide access to their physical radii, the internal shear forces acting on the quarks and their pressure distributions."*

In the DG_neutron, the core values of the DG energy density distribution for the co-centered electron are of the same sign as the energy-density shell values of the protonic-muon structures but of an almost infinitesimal value compared to the muonic values. At the electron-core radius the two energy density distributions are of opposite magnitudes and produce a composite neutral charge character ($Qneu$ = 0)(for radii greater than ro(electron)) and the modified g-factors discussed above.

4. CONCLUSIONS

It has been shown in the present work that the distorted-space, or distorted geometry (DG), model of matter, as applied to fundamental-particle (muon/anti-muon) constructs, can mimic the composite neutron and proton structures. The distorted-geometry structures exhibit non-Newtonian features wherein the core-region and shell-region fields of the structures do not behave functionally in an r^{-4} manner and terminate at zero at the radial origin (no singularity). This field behavior is a fundamental feature of these "distorted-space" structures; the field behavior exhibits r^{-4} , r^{-6} and other r^{-n} dependence in both the core and shell regions and is thereby able to account for, explain and mathematically elucidate "Newtonian"-, "weak"-and "strong"-fields."

REFERENCES

[1] Clifford, W.K., "On the space theory of matter" in Proc. Of the Cambridge Philosophical Society, 2, pp. 157-58, (1876).

[2] Ciufolini, I. and Wheeler, J. A., "Gravitation and Inertia", USA, Princeton University Press, (1996).

[3] Wheeler J. A., Phys. Rev., vol. 97, p.511, (1955).

[4] Wheeler J. A., "Logic, Methodology, and Philosophy of Science", Proc. 1960 International Congress, USA, Stanford University Press, p.361, (1962).

[5] Anderson, P.R.and Brill, D.R., Phys.Rev. , D56 4824-33, (1997)

[6] Perry, G.P.; Cooperstock, F.I. Class.Quant.Grav., 16 (1999)

[7] Sones, R.A., Quantum Geons, (2018) arXiv:gr-qc/0506011

[8] Stevens, K.A.; Schleich, K.; Witt, D.M., Class.Quant.Grav., 26:075012, (2009)

[9] Vollick, D.N., Class.Quant.Grav., 27:169701, (2010)

[10] Louko, J. J., Phys.: Conf. Ser., 222:012038, (2010)

[11] Koehler, D. R., "Geometric distortions and physical structure modeling" in Indian J. Phys., vol.87, p.1029 (2013). DOI 10.1007/s12648-013-0321-5 .

[12] Koehler, D. R., "The distorted universe: from neutrinos to the cosmos, the theory of nothingness", in Universe-neutrinos-cosmos-Nothingness-ebook, Kindle, ASIN B00TG26Q7Y, 2015.

[13] Tolman, R., "Relativistic electrodynamics" in Relativity, Thermodynamics and Cosmology, Mineola, NY, Dover, p.258, (1987)

[14] "2018 CODATA Value: electron mass in u". The NIST Reference on Constants, Units, and Uncertainty. NIST., (20 May 2019).

[15] Gell, Y. and Lichtenberger, D. B., "Quark model and the magnetic moments of proton and neutron" in Il Nuovo Cimento A., Vol. 61(1), series 10, pp 27-40, (1969) doi: 10.1007/BF02760010. S2CID123822660

[16] Alvarez, L.W. and Bloch, F., "Determination of the neutron moment in absolute nuclear magnetons" in Physical Review. 57 (2), pp. 111-122, (1940).

[17] Burkert, V.D., Elouadrhirim L.and Girod, F.X. , "The pressure distribution inside the proton " in Nature 557, pp.396-399, (2018). https://www.nature.com/articles/s41586-018-0060-z#auth-L_-Elouadrhiri

Competing Interests There are no competing interests for this paper

Author Contribution Statement The work and representation was provided by the sole author

Correspondence and requests for materials should be addressed to drkoehler.koehler@gmail.com

Figure Legends

Fig. 1 Electric-Field energy-density distribution function for distortion-1 ≡ down_quark (mass-energy = 9.269 me*c^2), distortion-2 ≡ electron and distortion_3 ≡ muon (mass-energy = 206.768 me*c^2) where $\boldsymbol{\rho F14} \equiv \boldsymbol{Fd_{14}}^2$ (see Eqs 12-15); logarithmic ordinate in J/m^3 units and logarithmic abscissa in meters.

Fig.2 Metrics and propagation-velocity factor for an electron structure; .uoo = 1.27394.

Fig.3 Mass-Energy-Density distribution-function surface-plots (two views) (linear radii and logarithmic amplitudes) for the geometric electron distortion.

Fig. 4 Radial-zero functions u_0 (from Eqs.(6)) relative to electric-charge values; *uE0* for the electrical $\boldsymbol{Td_2^2}$ function, *uM0* for the mass-energy-density $\boldsymbol{Td_4^4}$ function and *uB0* for the magnetic-energy-density $\boldsymbol{Td_1^1} + \boldsymbol{Td_2^2}$ function. Abscissa charge-values are displayed as a function of the index *Qq*. *uo(Qq)* is graphically used for the zero-radial-function *uo*. Also indicated is the E_field quantity, *u0_core* = *uE0(Qq* = 0), and a gravitational "black-hole *u0_bh*" value.

Fig.5 Field-Energy-Density distribution-functions; radii (logarithmic in meters) and amplitudes (logarithmic in joules/m^3) for the DG_geometric electron-distortions. EM_mag ≡ $\boldsymbol{Fd_{mag}}^2(\boldsymbol{electron})$ and EM_e ≡ $\boldsymbol{Fd_{14}}^2(\boldsymbol{electron})$**.**

Fig.6 Field-Energy-Density distribution-functions; radii (logarithmic in meters) and amplitudes (linear in joules/m^3) for the DG_geometric electron-distortions. EM_mag ≡ $\boldsymbol{Fd_{mag}}^2(\boldsymbol{electron})$ and EM_e ≡ $\boldsymbol{Fd_{14}}^2(\boldsymbol{electron})$**.**

Fig.7 Field-Energy-Density distribution-functions; radii (logarithmic in meters) and amplitudes (logarithmic in joules/m^3) for the DG_geometric distortions ***U_pro(r), U_elec(r)*** and ***U_neu(r).***